



AFRL-RZ-WP-TP-2008-2037

**EXPERIMENTAL STUDY OF CAVITY-STRUT
COMBUSTION IN SUPERSONIC FLOW (POSTPRINT)**

K. -Y. Hsu, Campbell D. Carter, M.R. Gruber, and T. Barhorst

**Propulsion Sciences Branch
Aerospace Propulsion Division**

JULY 2007

Approved for public release; distribution unlimited.

See additional restrictions described on inside pages

STINFO COPY

**AIR FORCE RESEARCH LABORATORY
PROPULSION DIRECTORATE
WRIGHT-PATTERSON AIR FORCE BASE, OH 45433-7251
AIR FORCE MATERIEL COMMAND
UNITED STATES AIR FORCE**

Experimental Study of Cavity-Strut Combustion in Supersonic Flow

K. -Y. Hsu*

Innovative Scientific Solutions, Inc.
2766 Indian Ripple Road
Dayton, OH 45440, USA

C. D. Carter,[†] M. R. Gruber,[†] and T. Barhorst[‡]

Air Force Research Laboratory (AFRL/PRAS)
Propulsion Directorate
1950 Fifth Street
Wright-Patterson AFB, OH 45433, USA

An experimental investigation of cavity-based flameholders with strut injectors in a supersonic flow is reported. In this ongoing research program, emphases are placed on understanding cavity-based flameholders and providing alternative methods for improving overall combustor performance in scramjet engines. Three different struts with fuel injectors are mounted near the cavity leading edge to study flame propagation and ignition of fuel in the core flow region. OH-PLIF is used to identify the flame zone around the cavity and strut-wake regions over a range of conditions. Shadowgraphy is used to capture the flow features around the strut and cavity. In-stream probing is conducted to characterize the flow features associated with the different strut configurations. Stagnation-temperature profiles are obtained for all struts operating over the same conditions in the combustor-flow study. Two cavity fueling schemes are used to compare flameholder performance. Direct cavity air injection is found to improve combustion significantly. For each strut, upstream and downstream fueling schemes are compared over a range of conditions. Overall, successful combustion is observed in the strut-wake region using upstream strut-fueling schemes for the three struts employed in this study.

I. Introduction

Cavity-based flameholders are commonly used in hydrocarbon-fueled scramjet combustors; however, detailed information concerning the behavior of these devices, their optimal shape and fueling strategies, combustion stability, interactions with disturbances in the main air flow (i.e., shock trains or shock-boundary layer interactions), and capability of ignition and sustained main combustion is largely unavailable in the existing literature. Studies^{1,2,3,4,5,6} of cavity-based flameholders in supersonic flows conducted at AFRL/PRA have illustrated that the combustion around a flameholder can be optimized with proper fueling.

Development of a flameholder that exhibits stable operation over a broad range of conditions and is capable of effective ignition and sustained main combustion at lower Mach numbers requires study of the coupling mechanism between the flameholder and the main air/fuel streams. The shear-layer formed at the interface between the cavity and main stream has been identified as a critical region in the development of efficient flameholders in scramjet engines. This shear layer plays an important role in transferring mass and energy in and out of the cavity. The air entrained into the cavity is a direct result of the shear-layer interaction with the cavity, which directly affects the mixing and stoichiometry inside the cavity. The exchange of species and energy between the main flow and the cavity can directly impact the operating limit of the flameholder and ignition of the main combustion.

* Sr. Research Scientist, 2776 Indian Ripple Road, Dayton, OH 45440, AIAA Associate Fellow

[†] Sr. Aerospace Engineer, AFRL/PRAS, 1950 Fifth Street, WPAFB, OH 45433, AIAA Associate Fellow

[‡] Engineer, AFRL/PRAS, 1950 Fifth Street, WPAFB, OH 45433, AIAA Member

Fuel injection in the scramjet combustor has been studied for decades, with the main emphasis being placed on mixing and efficient combustion. To achieve fueling in the supersonic core region, strut injectors have been used to improve distribution and mixing in supersonic combustors^{7,8,9,10}.

The main objective of this study is to examine the coupling between the cavity and the strut-injected fuel and the potential to improve the combustion in a scramjet engine. Conventional and advanced diagnostics are used to characterize the interactions between the cavity and the wake region created by struts.

II. Experimental Description

This experimental study of a cavity-based flameholder was conducted in a supersonic research facility (Research Cell 19) located at the Air Force Research Laboratory, Propulsion Directorate. Details of the facility are discussed in a previous paper. Continuous Mach-2 air flow was achieved via an asymmetric two-dimensional facility nozzle that is connected upstream of the test section. Cavity flameholder tests were conducted in a rectangular test section with optical windows located in three walls. The bottom wall consists of modular hardware that allows various test configurations to be installed and tested. The test section has a 17.78-cm-long constant-area section (5.08 cm. high by 15.24 cm wide), followed by a 2.5-degree divergence on the bottom wall. The cavity flameholder and strut injector are located on the bottom wall of the test section (see Fig. 1).

The baseline cavity and three different strut injectors were installed upstream of cavity, as illustrated in Fig. 1. The cavity extends 15.24 cm in the spanwise direction (z), with a 90-degree leading edge and 22.5-degree ramp at the trailing edge. The cavity is 1.65 cm. deep, and the length of the cavity floor is 4.57 cm. Three rows of injection ports are located along the cavity ramp for fuel and air injection. The middle row has 10 injectors, and the top and bottom rows have 11 injectors each. A separate manifold was used to feed each row independently. All injection ports are parallel to the cavity floor and 0.16 cm in diameter. Spark Plugs installed on the cavity floor were used for ignition.

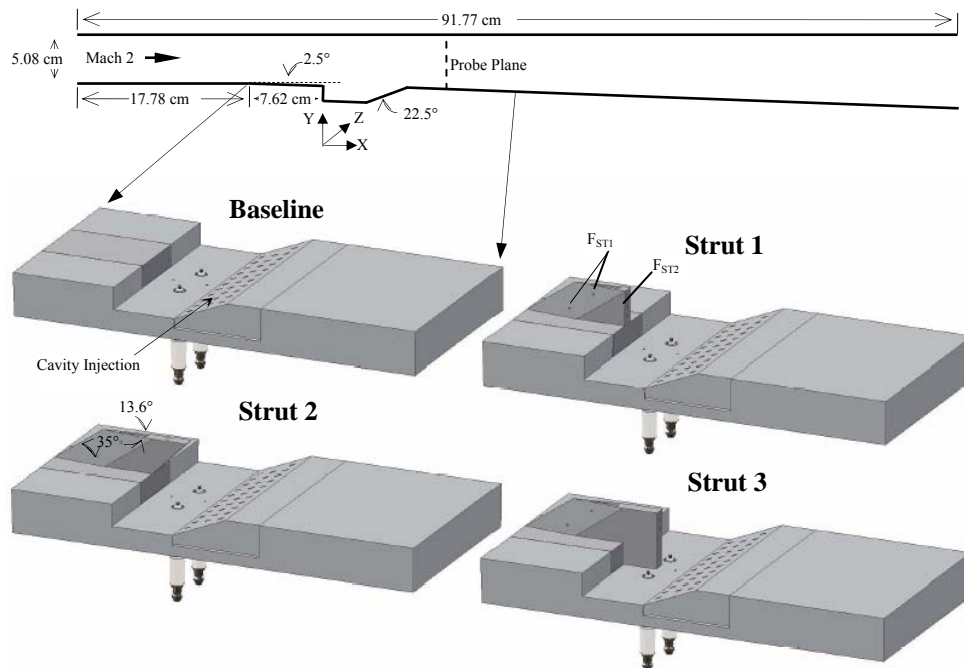


Figure 1. Configurations of cavity and strut injectors.

The three struts have a 35-degree sweep angle and a 13.6-degree compression angle at the leading edge. The struts are installed flush with the floor upstream of the cavity, with the leading edge located 7.62 cm upstream of the cavity leading edge, as shown in Fig. 1. The struts are 2.54 cm tall and 0.95 cm wide at the base. The main difference among the struts is the length and shape of the aft body. Strut 1 has a vertical trailing edge that is aligned with cavity leading edge. Strut 2 has a 45-degree slanted trailing edge that extends over the top of the cavity. Strut 3

is similar to Strut 1, except that it is 2.54 cm longer and extends to the floor of the cavity. Two fuel-injection schemes are employed for each strut. Three upstream fuel injectors (F_{ST1}) are located at the leading edge, with two on one side and one on the other side, with a vertical spacing of 0.64 cm. Three downstream fuel injectors (F_{ST2}) are located at the base of the strut with a vertical spacing of 0.64 cm. All injection ports are 0.16 cm in diameter, with two independent internal manifolds.

Combustion tests were conducted at Mach 2, with stagnation conditions of $P_0 = 345 - 483$ kPa and $T_0 = 590$ K. For non-reacting flow studies, the stagnation temperature was set at $T_0 = 294$ K. Separate control/metering of fuel (ethylene) and air was used for cavity and strut fuel injections. Two critical venturi nozzles were employed to meter the ethylene flowrate. A mass flow controller was used to control and meter the cavity air injection.

Planar Laser-Induced Fluorescence (PLIF) was used to identify the OH distribution around the cavity and strut-wake regions over a range of injection conditions. Detailed descriptions of the OH-PLIF technique were presented in a previous paper. Shadowgraphy was also used to capture the flow features around the strut and cavity.

Probe measurements were made to obtain quantitative flow information. Probe data (Pitot and cone-static pressures and total temperature) were collected over a plane normal to the flow direction at a fixed axial location 4.45 cm downstream of the cavity. The probe was inserted through a movable probe wall and attached to a spanwise (z) traversing system. The probe wall was attached to the optical table, which was located below the test section to allow traversing in the y direction. By controlling the traverse system and optical table, one can collect two-dimensional (y-z plane) probe data normal to the flow direction with any desired resolution. For non-reacting flow, probe data were collected over a fixed spatial domain ($0 \leq z \leq 8.89$ cm and $0 \leq y \leq 5.08$ cm), with 0.25-cm resolution for both y and z directions. For the reacting-flow experiment, only the total temperature probe was used to collect temperature-field data with reduced resolutions as compared to the non-reacting case (0.51 cm x 0.51 cm). For non-reacting flow, flow quantities such as total pressure and temperature, static pressure, Mach number, and density can be reduced from raw probe data using a custom data-reduction routine.

III. Results and Discussion

A. Baseline Cavity

For a baseline cavity flameholder with fueling from the ramp, the side-view OH distributions along the symmetric plane were recorded, as illustrated in Fig. 2. Ensemble-averaged (EA) and standard-deviation (SD) images were processed from multiple OH images for a range of cavity fuel flowrates. At low cavity fueling, the combustion filled almost the entire cavity region. Increasing the cavity fueling resulted in a fuel-rich region located near the leading edge of the cavity. With sufficient heat release, excess fuel was burned in the shear layer over the cavity. The fuel-rich region is caused by insufficient air being entrained from the main air stream to complete the combustion at higher cavity fueling. Higher fluctuations of OH signal were observed close to the cavity floor and the leading edge of the cavity. It should be mentioned that the flow field and combustion in the cavity are highly three dimensional and dynamic in nature. To improve the cavity combustion and broaden the operation range, air was injected directly into the cavity (see Fig. 1) using a row of injection ports below the fuel ports on the ramp. Figure 3 displays OH images for constant cavity fueling (58 slpm) and a range of cavity air flows. Clearly, the fuel-rich region at the leading edge was reduced by supplying additional direct-inject cavity air; however, a region of low OH signal was developed in the mid-region of the cavity. It is thought that switching the fuel ports closer to the cavity floor and

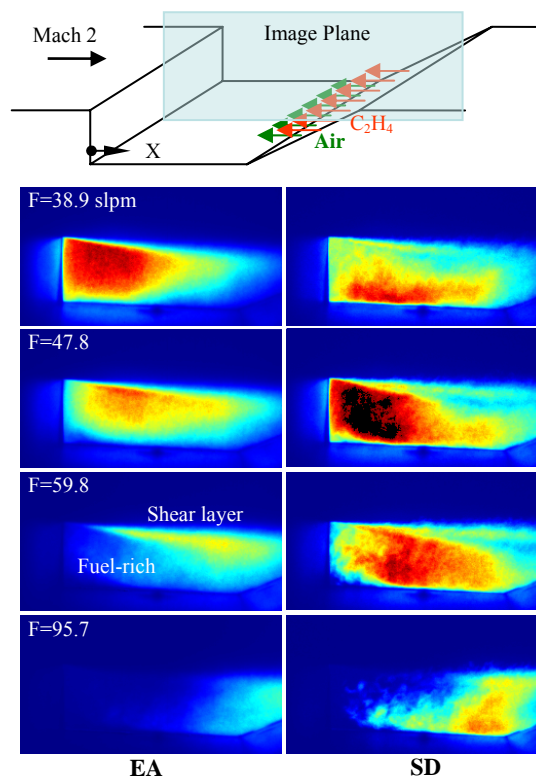


Figure 2. EA and SD of OH along symmetric plane with increasing cavity fuel.

injecting air above the fuel will improve the combustion volume and heat release.

Two cavity fuel- and air-injection schemes (see Fig. 4) were used to compare the performance of baseline cavity combustion. One method involves injecting fuel close to the cavity floor and injecting air slightly above the fuel jets. Another method involves reversing the arrangement by injecting air closer to the cavity floor. Figure 4 shows the ensemble-average of OH images using same color table (end-view) for the two injection schemes, collected at different axial (x) locations. The cavity leading edge was used as the reference for the axial coordinate. The image covers a spatial area 8.89 cm wide by 5.08 cm high, and the left side of each image corresponds to the left side-wall. In general, a distributed combustion zone inside the cavity is evident, regardless of the injection scheme employed, and instantaneous OH images reveal the dynamic features of cavity combustion. Weak combustion along the centerline is evident for both fueling schemes. Fueling closer to the floor of the cavity provides a slightly broader flame zone. The addition of air directly into the cavity broadens the combustion zone, especially in the shear-layer region.

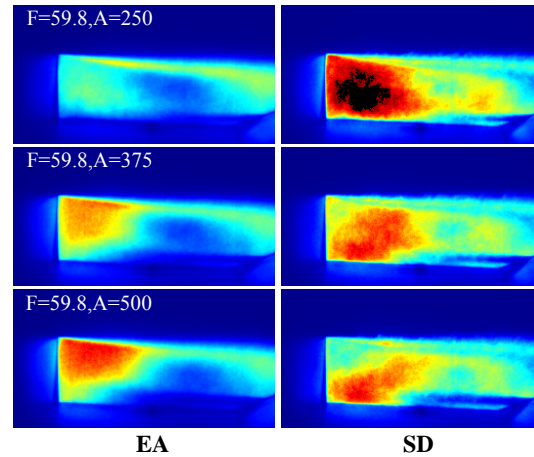


Figure 3. OH distribution along symmetric plane with various cavity air flowrates at cavity fuel of 59.8 slpm.

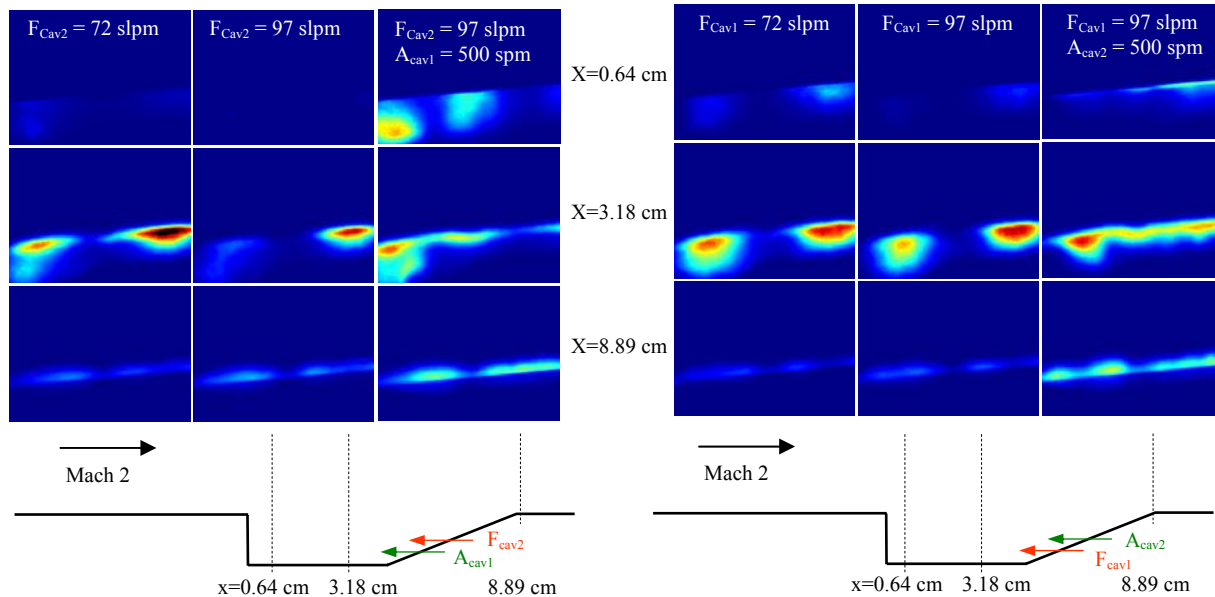


Figure 4. End-views of OH distributions for two cavity injection schemes.

B. Strut-Cavity

1. Flame Emission Imaging

For a basic cavity flameholder, the shear layer over the top and downstream of the cavity is the region that can ignite the main fuel effectively. For this study, the interaction between the cavity and the wake created by the strut is used to enhance the region of ignition and flameholding of the main fuel. Figure 5 displays flame images of Strut 2 for two different fueling schemes at a constant cavity fueling condition. The flame behind the strut was evident with

cavity fuel only. The low-pressure wake region behind the strut was found to be effective in extending the combustion out of the cavity region for improved flameholding capability. The flame propagated from the cavity fills the full strut height (2.54 cm). For upstream strut fuel injection (F_{ST1}), the combustion zone behind the strut extends farther downstream with increased strut fuel and is more evident near the tip of the strut. It is thought that the sweep and compression angles at the leading edge of the strut turn the flow upward, causing more strut fuel to be distributed toward the top of the strut. Combustion was found to be less intense using the downstream strut fueling (F_{ST2}) scheme, as illustrated in Fig. 5. The downstream strut injection modifies the flow and stoichiometry in the wake region where the cavity flame propagates. The area of combustion is reduced significantly with increasing

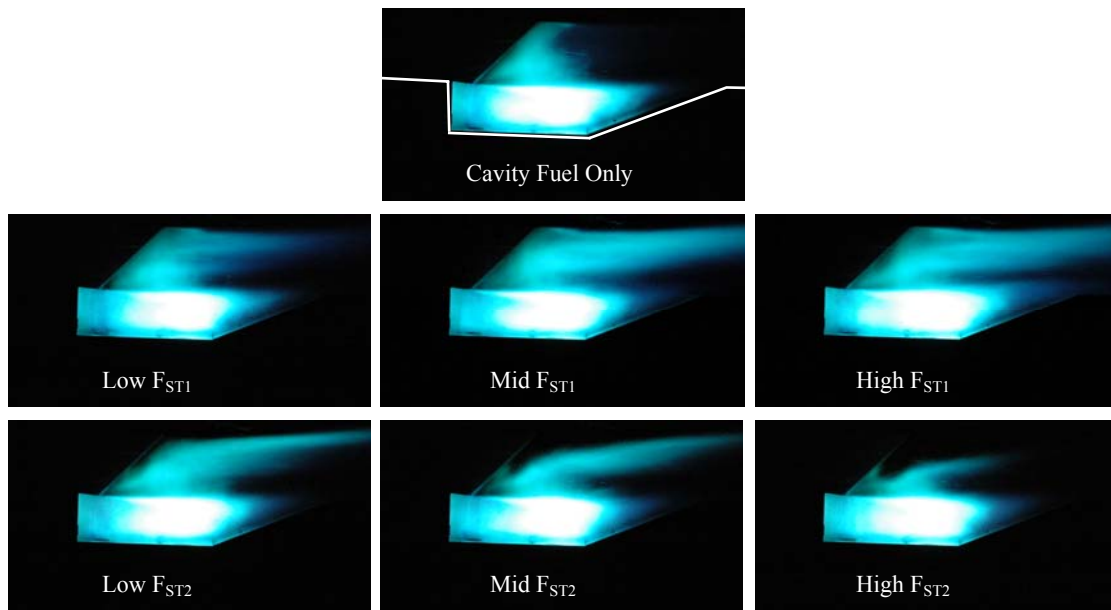


Figure 5. Flame images of Strut 2 with upstream (F_{ST1}) and downstream (F_{ST2}) fueling.

downstream strut fuel. On the other hand, upstream strut fueling provides better mixing and sustains more combustion in the wake region.

Figure 6 shows a comparison of flame images of cavity-strut combustion using three different struts operated over a range of conditions. At medium cavity fuel loading (74 slpm), the combustion zone was found to extend throughout the cavity and propagate into the wake region behind the strut. As cavity fueling increases, the flame extends farther downstream in both the cavity and the strut-wake regions. In the mid-height region behind Strut Configuration 2, the OH signal is weak, which suggests a locally fuel-rich region. When air is directly injected into the cavity, the flame appears to be more intense with reduced flame length behind the strut, which also suggests that the strut wake is mainly fuel rich. The addition of cavity air also reduced the stoichiometry behind Strut Configuration 2. At a moderate upstream strut fueling (F_{ST1}), the increased combustion zone behind the struts is evident, especially with regard to the flame length. At the same cavity and strut fueling condition, the strut flame appears to extend farther downstream in the Strut 2 and Strut 3 configurations. Combustion behind Struts 1 and 2 was improved by introducing higher cavity air. All three struts provide a low-pressure wake region for flame propagation and flameholding. It should be mentioned that the flame emission images shown in Figs. 5 and 6 reflect a line-of-sight average.

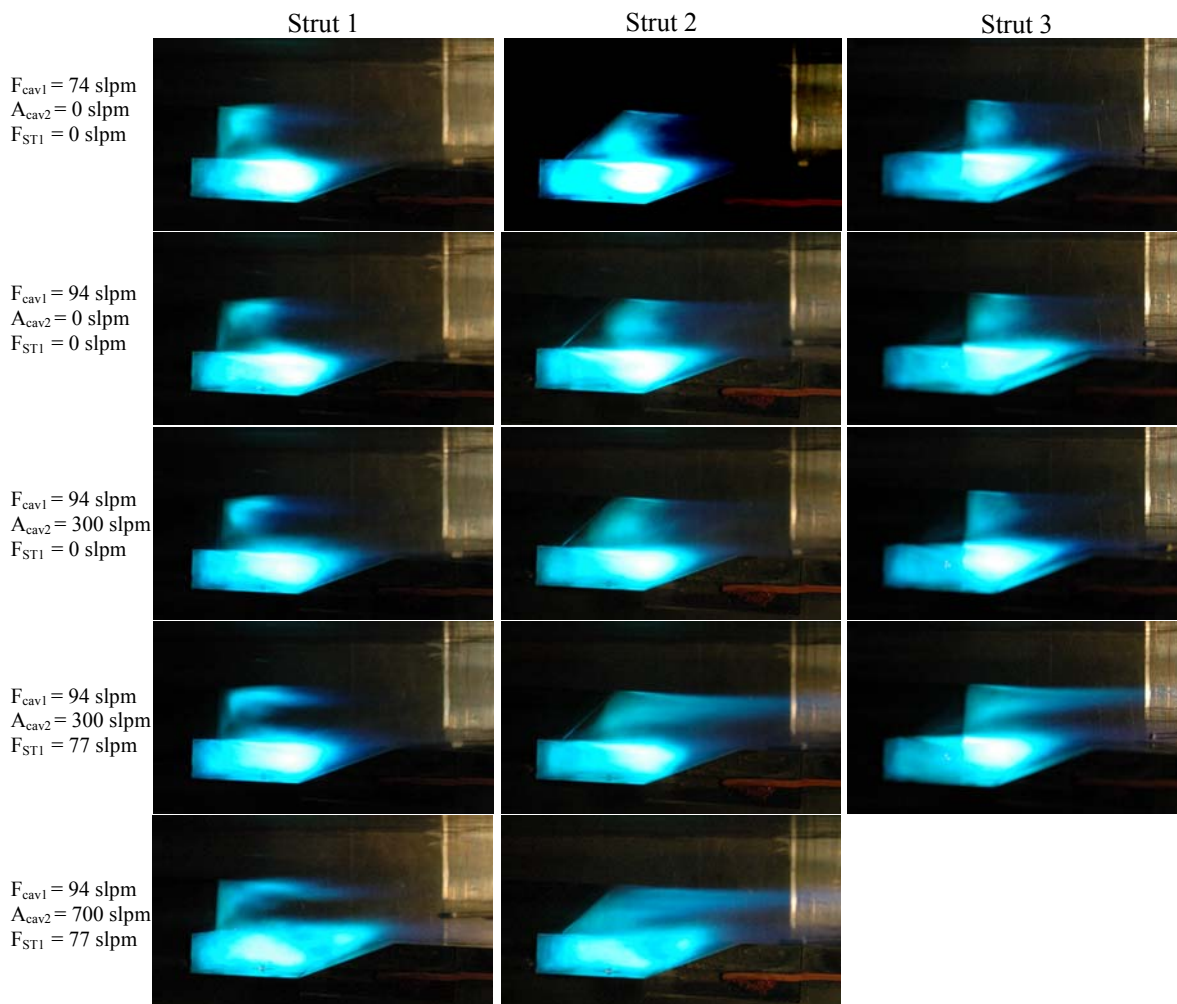


Figure 6. Flame images of three different struts at various conditions.

2. OH PLIF

The PLIF technique was used to measure spatially resolved planar distributions of OH normal to the streamwise direction. Multiple OH images were collected at various fueling conditions and axial locations for each strut combustion case. Ensemble-averages of multiple images were processed with the same false color table for the following discussions. Figure 7 illustrates OH distributions with Strut Configuration 1 collected at various cavity and strut fueling at three axial locations ($x = 0.64, 3.18$, and 8.89 cm). Results of two different cavity fuel and air schemes are shown in Figs. 7a and 7b. When the cavity fuel was injected closer to the cavity floor, as illustrated Fig. 7a, strong OH intensity was observed in the strut-wake regions. A shear-layer flame was also evident at $x = 0.64$ cm. The OH intensity decreased with increasing cavity fuel at all three axial locations. The strut wake region became excessively fuel-rich as upstream strut fuel (F_{ST1}) was introduced. The addition of cavity air significantly improved the cavity-strut combustion, as illustrated in the figure. When the cavity fuel was injected above the cavity air, as shown in Fig. 7b, the OH intensity was greater as compared to that with the other cavity fueling scheme. The cavity flame seemed to be more intense behind the strut wake. A higher intensity of OH was observed at a downstream location ($x = 8.89$ cm) with this cavity fueling scheme. In general, a longer residence time and more efficient mixing are achieved when fueling closer to the cavity floor (ref. Fig. 7a). When fuel is injected away from cavity floor (ref. Fig. 7b), most of the fuel is burned farther downstream because of lower residence time and poorer mixing. The

distribution of OH with respect to the fueling follows the same trend for both injection schemes. Regardless of the cavity injection scheme, the OH distribution is triangular in shape and becomes narrower toward the core flow. This is probably due to the flow expansion toward the centerline, immediately downstream of the strut. It should be mentioned that a strong counter-rotating structure was observed at the tip of the strut-wake for both injection schemes. For this strut configuration, the velocity gradient is expected to be higher near the top of the cavity because of stronger flow expansion.

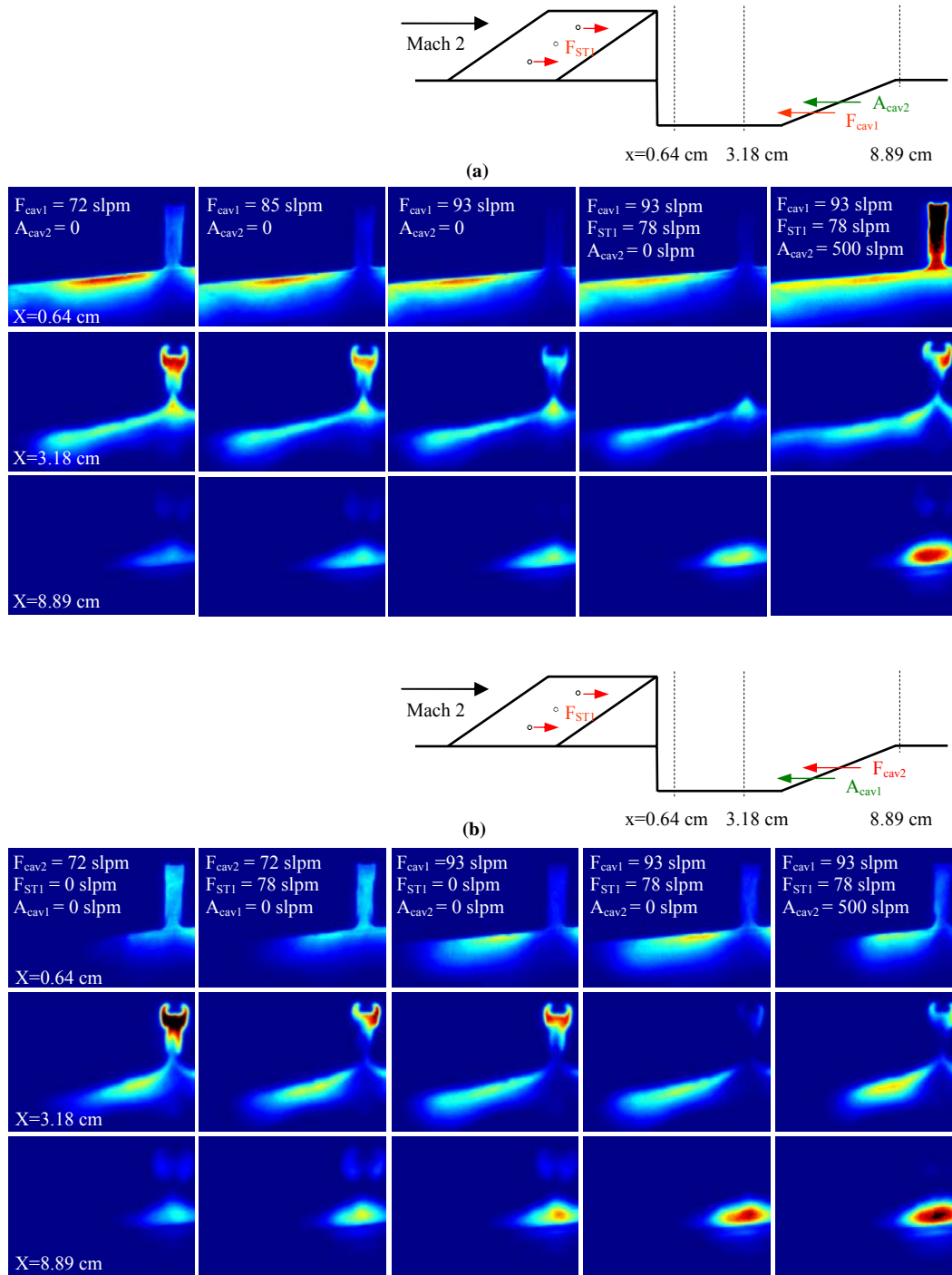


Figure 7. OH distributions using Strut 1 at various cavity loadings.

For Strut Configuration 2, similar trends were observed for the two cavity fuel-air injection schemes. Figure 8 shows the OH distributions for two strut fueling schemes with the same cavity injection. Without additional cavity air, the strut wake becomes excessively fuel rich (lower OH intensity), with increasing upstream strut fuel (F_{ST1}). The asymmetry of the OH in the wake region is due to the asymmetric upstream strut injection. When the fuel was injected from the strut base (F_{ST2}), the combustion in the strut wake was diminished, as shown Fig. 8b. The OH

intensity in the wake region decreases significantly with increasing fuel flowrate for F_{ST2} . Injecting fuel from the base of the strut disrupts the low-pressure wake region that is responsible for propagating cavity combustion toward the core flow. The addition of poorly mixed fuel directly to the wake region reduces the performance of strut combustion.

OH distributions of Strut 3 combustion are shown in Figs. 9 and 10. In Fig. 9 the two different cavity injections with Strut 3 installed are compared. When the cavity fuel was injected closer to the cavity floor, fairly uniformly distributed OH was observed at $x = 0.64$ cm (see Fig. 9a). Higher OH intensity is observed in the strut wake region ($x = 3.18$ cm), and the intensity decreases at $x = 8.89$ cm. Figure 9b shows the OH distribution when the cavity fuel was injected farther away from cavity floor. While almost no OH signal was observed in the strut wake region ($x = 3.18$ cm), stronger OH was observed at $x = 8.89$ cm. The residence time of the cavity mixture was apparently shorter along the centerline because of the extended strut length. Combustion was delayed, with stronger combustion occurring farther downstream.

Figure 10 compares the OH distributions for two strut fueling schemes employing the same cavity injection method. Upstream strut injection provides better mixing and combustion in the wake region. The addition of cavity air improves the cavity and strut combustion significantly. It should be mentioned that the wake structure is similar for Struts 2 and 3. Strut 1 has a very distinct wake structure as compared to the others.

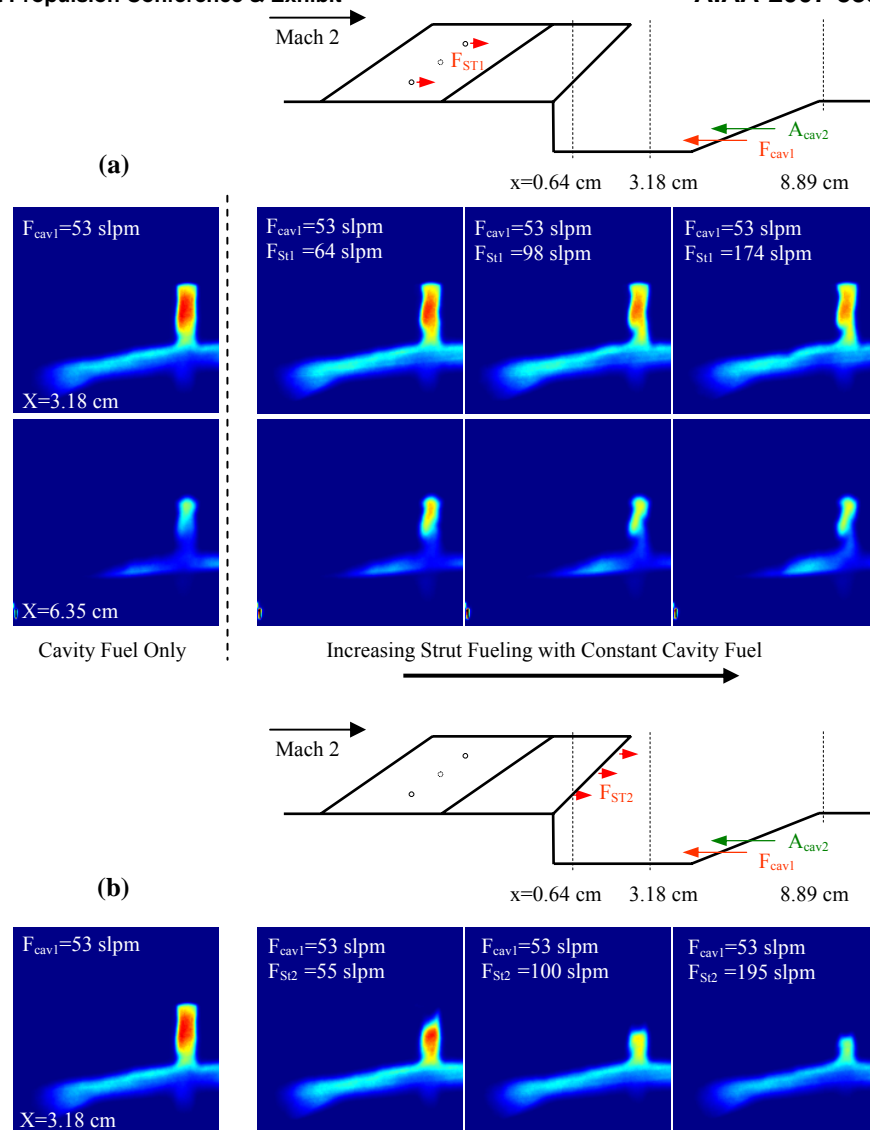


Figure 8. Effects of Strut 2 fueling schemes (upstream vs. downstream).

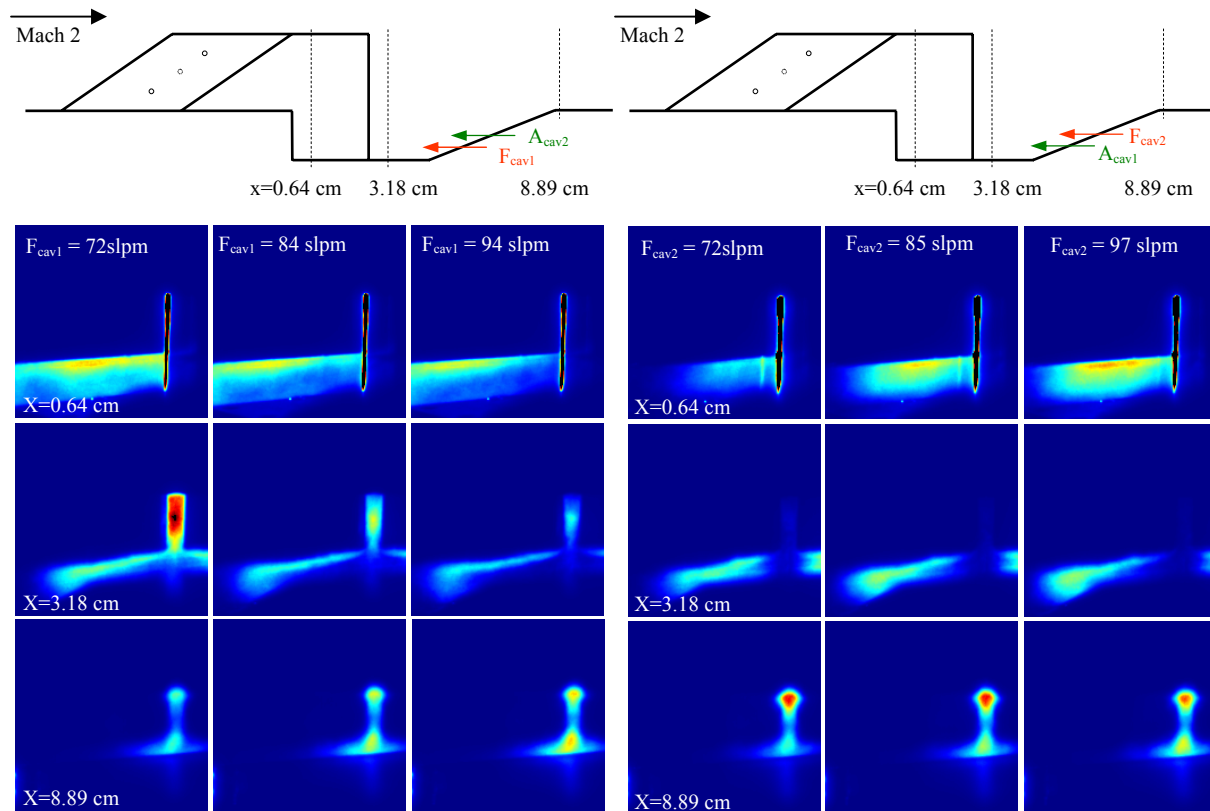


Figure 9. Effects of cavity fueling with Strut 3.

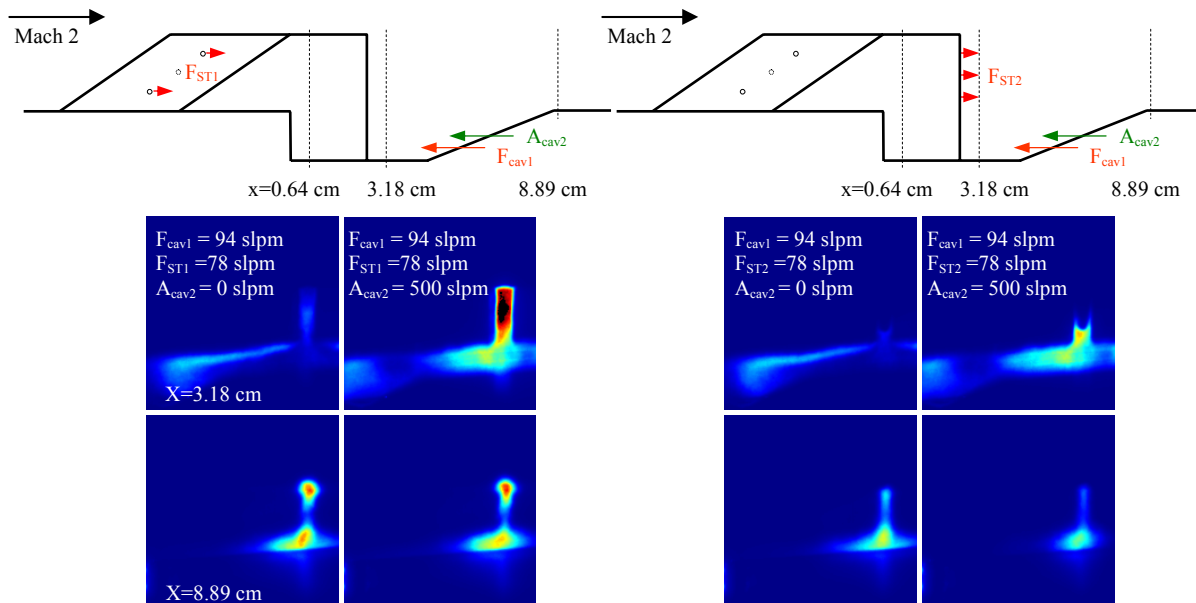


Figure 10. Effects of Strut 2 fueling schemes.

3. Shadowgraphy

Three different struts installed upstream of the cavity introduce different flow patterns in the wake region. The main difference in these three struts is the shape of the aft body. Flow features of the wake region are illustrated in Fig. 11 by shadowgraph images. For the baseline cavity, flow expansion was observed at the divergent location (i) along the bottom wall, 7.62 cm upstream of the cavity. Another weak expansion wave was located at the cavity leading edge (ii). The shear layer can be clearly identified along the bottom wall and over the cavity. A series of weak recompression waves (iii) emanating from the cavity ramp was observed. A distinct compression wave (iv) can be observed just upstream of each strut. The flow compressed along the leading edge of the strut and was diverted from the bottom wall. This flow diversion is thought to be the mechanism for transporting upstream-injected strut fuel toward the tip of the strut, especially for Strut 1. A wave generated near the tip of the strut was also observed for all three struts, and this wave region is larger for Strut 1. Strut 1 is the shortest (in length) of the three, and the flow expansion at the base of Strut 1 should be much greater as compared to that of the others. The velocity gradient along the perimeter of the base of Strut 1 should also be greater because of the faster flow expansion as compared to that of Strut 2 and Strut 3 (see Fig. 1). The structure generated at the top of Strut 1, as shown in Figs. 7 and 11, is probably a result of the unique flow structure behind this strut.

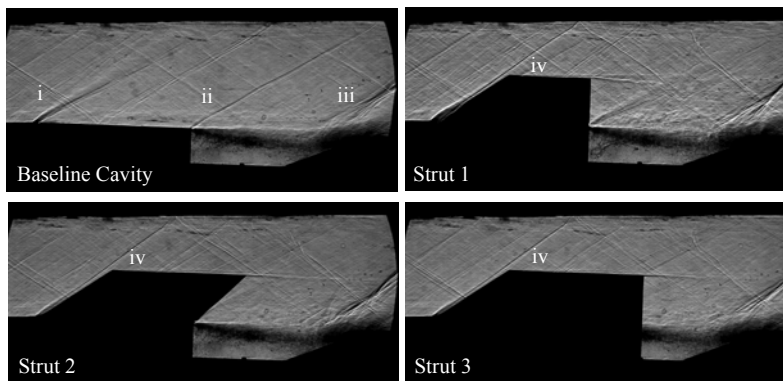


Figure 11. Flow features illustrated by shadowgraph images.

4. Probe Data

A total temperature probe was used to collect temperature profiles for all three struts operating over a range of reacting flow conditions. Figure 12 shows temperature contours for all three struts for direct comparison. Although Strut 1 produces a wider flame zone in the wake of strut, the peak temperature is lower as compared to Struts 2 and 3 operated at similar conditions. Combustion downstream of the cavity was concentrated near the centerline as a result of the influence of the strut. The combustion zones of the strut-wake and cavity regions seem disconnected in Strut 1, which is consistent with the flame images shown in Figs. 6 and 7. Similar temperature contours were observed for Struts 2 and 3 operated at similar conditions, except that Strut 2 exhibited much higher temperature in the core of the strut wake and cavity centerline at higher fuel and air flows. Strut 2 also has a larger wake combustion region, as compared to Strut 3. A neck-down region appears to connect the cavity and strut-wake along the centerline for all three struts. This region probably results from flow expansion toward the centerline near the base of the aft body.

Probe measurements were also conducted in non-reacting flow for all three struts. Basic flow information was reduced from raw probe data that were collected at the same axial location as that discussed in Fig. 12. Figure 13 show contours of Mach number, total pressure, and stream thrust for all three struts. The strut wake region has both low total pressure and low Mach number, providing a region for flame propagation from the cavity and sustained combustion for upstream strut fueling. The main difference in the Mach contours for all of the struts is in the shape of the wakes. Strut 1 appears to have the largest low-Mach wake region. The shape of the total-pressure contour is similar to that of the Mach contours for the corresponding strut configuration. Strut 3 appears to have the lowest total pressure in the strut-wake region because of its greater length (creating more flow losses). The wake shapes correlate well with the total-temperature contours obtained from reacting cases (see Fig. 12). The flow structure created by the strut and its interaction with the cavity flow is a deciding factor in how well the fuel is mixed and burned. Stream thrust is calculated by $m \cdot V + P \cdot A$ at each spatial location, where m is the mass flux, V the axial velocity, P the static pressure, and A the area. Strut 1 has a slightly higher stream thrust distribution than the other

struts. Spatial-integrated stream thrust is also slightly larger for Strut 1, but the difference among the struts is negligible.

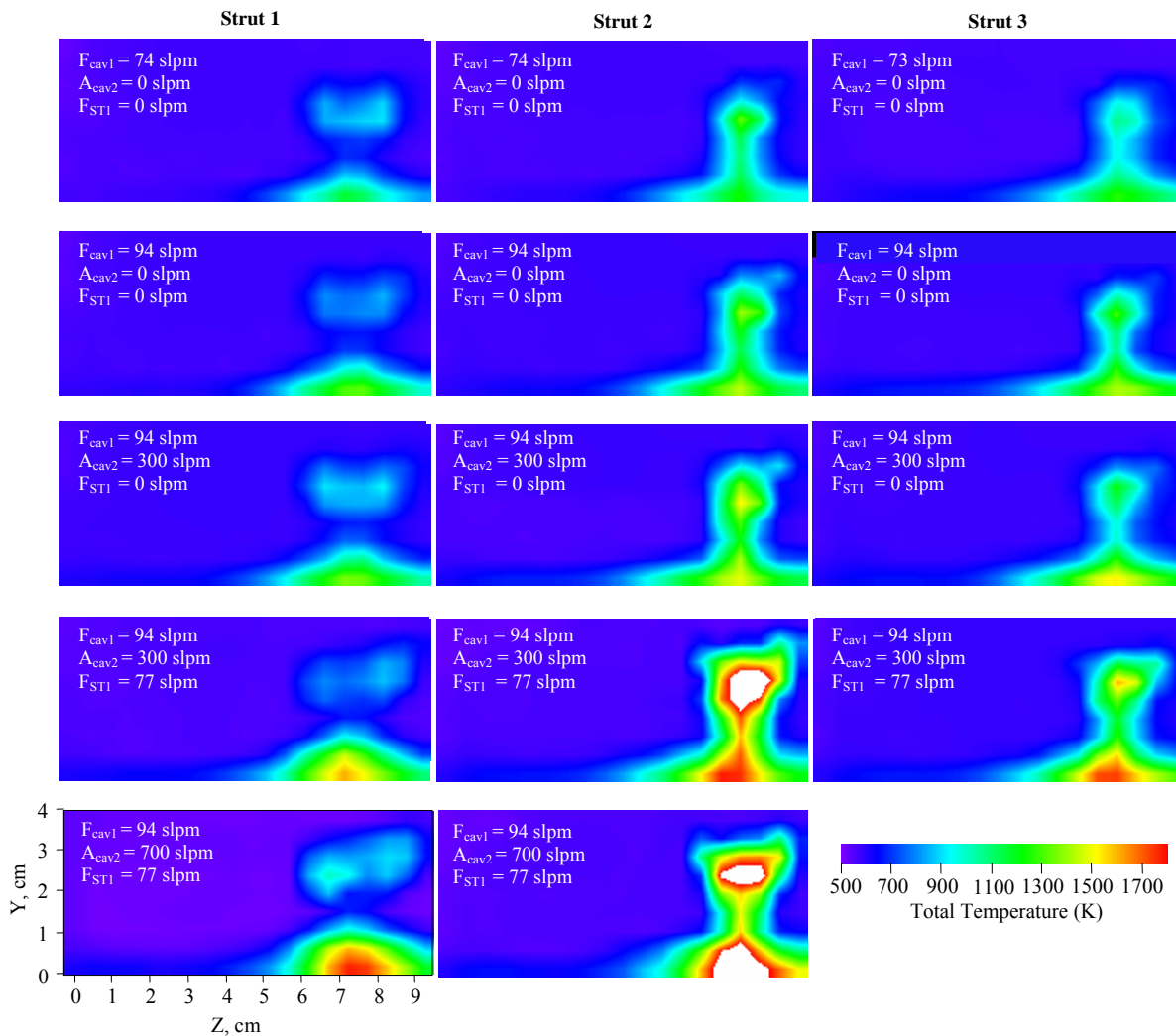


Figure 12. Temperature distributions at various conditions, measured 4.45 cm downstream of cavity.

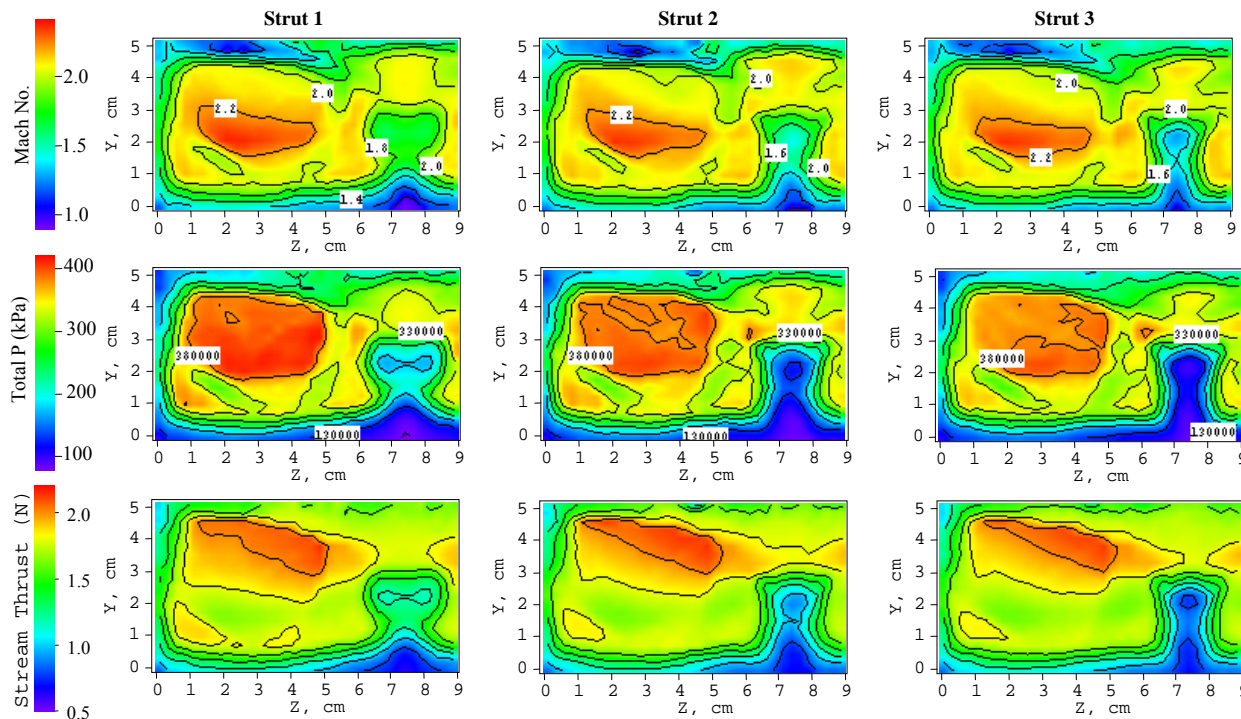


Figure 13. Contours of Mach number, total pressure, and stream thrust for three struts in non-reacting flow.

IV. Conclusion

Slight differences in flame distribution were observed for the two cavity fueling schemes employed in this study. Injecting the cavity fuel closer to the floor seems to provide better performance due to improved mixing and residence time.

In addition, three different strut injectors installed upstream of a cavity flameholder were evaluated as an alternative method for improving ignition and sustaining main combustion in a supersonic flowfield. Fuel injected upstream along the strut face was burned more effectively for all three struts tested. Different shapes of the strut wake were observed as a result of the modification of the flowfield around the strut and cavity regions. The addition of fuel directly in the wake of the strut creates a fuel-rich zone that inhibits the effective burning of the strut fuel and disrupts the wake flow. Direct cavity air injection improves combustion in the cavity and strut-wake regions dramatically, which potentially broadens the operation range of the cavity flameholder.

In-stream probe measurements were conducted for both reacting and non-reacting cases for each strut-cavity. For the reacting cases, higher temperatures were observed for Strut Configuration 2 at higher fuel and cavity air flows. The basic flow properties of each strut were also reduced from probe data collected at non-reacting conditions. Strut 1 appears to have a slightly larger wake than the others. However, the difference in the integrated stream thrust was negligible for the three struts.

V. Future Plans

To understand the flow interactions in the strut-cavity region, Particle Imaging Velocimetry (PIV) will be used to examine the complex flowfield for all struts. New struts of shorter length have been fabricated for study with a view toward further improving strut combustion with less flow losses.

Acknowledgements

American Institute of Aeronautics and Astronautics

This work was sponsored by the AFRL Propulsion Directorate under Contract F33615-03-D-2327. The authors would like to thank Mr. Robert Behdadnia for his support. The assistance of Messrs. G. Streby, D. Schommer, W. Terry, and Lt. B. Brantly in preparing and conducting experiments is also appreciated. The support of the Research Air Facility of AFRL/PR is also acknowledged.

References

-
- ¹ M. Gruber, J. Donbar, C. Carter, and K.-Y. Hsu, "Mixing and Combustion Studies using Cavity Based Flameholder in a Supersonic Flow," Presented at ISABE Meeting, ISABE-2003-1204, Cleveland, OH, 2003.
 - ² M. R. Gruber, J. M. Donbar, C. D. Carter, and K.-Y. Hsu, "Mixing and Combustion Studies Using Cavity-Based Flameholders in a Supersonic Flow," *Journal of Propulsion and Power*, Vol. 20, No. 5, pp. 769-778, 2004.
 - ³ C. C. Rasmussen, J. F. Driscoll, C. D. Carter, and K.-Y. Hsu, "Characteristics of Cavity-Stabilized Flame in a Supersonic Flow," Technical Note, *Journal of Propulsion and Power*, Vol. 21, No. 4, pp. 765-768, 2005.
 - ⁴ W. Allen, P. King, C. Carter, M. Gruber, and K.-Y. Hsu, "Fuel-Air Injection Effects on Combustion in Cavity-Based Flameholders in a Supersonic Flow," AIAA Paper 2005-4105, Presented at 41st AIAA/ASME/SAE/ASEE Joint Propulsion Conference and Exhibit, Tucson, AZ, 2005.
 - ⁵ S. Edens, P. King, M. Gruber, and K.-Y. Hsu, "Cavity-Based Flameholder for a Supersonic Combustor," AIAA Paper 2006-4861, Presented at 42nd AIAA/ASME/SAE/ASEE Joint Propulsion Conference and Exhibit, Sacramento, CA, 2006.
 - ⁶ D. Montes, P. King, M. Gruber, C. Carter, and K.-Y. Hsu, "Mixing Effects of Pylon-Aided Fuel Injection Located Upstream of a Flameholding Cavity in Supersonic Flow," AIAA Paper 2005-3913, Presented at 41st AIAA/ASME/SAE/ASEE Joint Propulsion Conference and Exhibit, Tucson, AZ, 2005.
 - ⁷ D. Bogdanoff, "Advanced Injection and Mixing Techniques for Scramjet Combustors," *Journal of Propulsion and Power*, Vol. 10, No. 2, pp. 183-190, 1994.
 - ⁸ T. Sunami, P. Marge, A. Bresson, F. Grisch, M. Orin, and M. Koder, "AIAA Paper 2005-3304, Presented at AIAA/CIRA 13th International Space Planes and Hypersonics Systems and Technologies.
 - ⁹ S. Tomioka, A. Murakami, K. Kudo, and T. Mitani, "Combustion Tests of a Staged Supersonic Combustor with Strut," *Journal of Propulsion and Power*, Vol. 17, No. 2, pp. 290-300, 2001.
 - ¹⁰ S. Desikan and K. Job, "Mixing Studies in Supersonic Flow Employing Strut Bases Hypermixers," AIAA Paper 2005-3643, Presented at 41st AIAA/ASME/SAE/ASEE Joint Propulsion Conference and Exhibit, Tucson, AZ, 2005.